Title

Efficient CRISPR/Cas9-mediated genome editing in the European corn borer, *Ostrinia nubilalis*

Running Title

Genome editing in corn borers

Authors and Affiliations

Jacob N. Dayton*, Tammy T. Tran, Elisa Saint-Denis, & Erik B. Dopman

Tufts University, Department of Biology, 200 Boston Avenue Suite 4700, Medford, MA, USA

*Corresponding Author: jacob.dayton@tufts.edu

Data Availability Statement

All sequence and database files used in the present study are provided or cited within the text; any biological data not provided is available upon reasonable request.

Funding Statement

This research was supported by grants from the Louis Stokes Alliances for Minority Participation for T.T.T. and Tufts University Undergraduate Research Fund for T.T.T. and E.S.D.. E.B.D. acknowledges support from the National Science Foundation (Award Number 2416175) and Tufts University.

Conflict of Interest Disclosure

The authors declare no conflict of interest.

Efficient CRISPR/Cas9-mediated genome editing in the European corn borer, *Ostrinia nubilalis*

Jacob N. Dayton, Tammy T. Tran, Elisa Saint-Denis, & Erik B. Dopman

Tufts University, Department of Biology, 200 Boston Avenue Suite 4700, Medford, MA, USA

*Corresponding Author: jacob.dayton@tufts.edu

Acknowledgements

We thank K. McLaughlin for access to critical microinjection equipment and F. Koutroumpa, Y. Yue, & A. Murray for helpful discussions. We thank S. Mirkin, B. Trimmer, M. Meuti, S. Zhan, & two anonymous reviewers for thoughtful feedback that improved the manuscript.

Abstract

The European corn borer (*Ostrinia nubilalis*) is an agricultural pest and burgeoning model for research on speciation, seasonal adaptation, and insect resistance management. Although previous work in *O. nubilalis* has identified genes associated with differences in life cycle, reproduction, and resistance to *Bt* toxins, the general lack of a robust gene-editing protocol for *O. nubilalis* has been a barrier to functional validation of candidate genes. Here, we demonstrate an efficient and practical methodology for heritable gene mutagenesis in *O. nubilalis* using the CRISPR/Cas9 genome editing system. Precise loss-of-function (LOF) mutations were generated at two circadian clock genes, *period* (*per*) and *pigment-dispersing factor receptor* (*pdfr*), and a developmental gene, *prothoracicotropic hormone* (*ptth*). Precluding the need for a visible genetic marker, gene-editing efficiency remained high across different single guide RNAs (sgRNA) and germline transmission of mutations to F_1 offspring approached 100%. When single or dual sgRNAs were injected at a high concentration, gene-specific phenotypic differences in behavior and development were identified in F_0 mutants.

Specifically, F_0 gene mutants demonstrated that PER, but not PDFR, is essential for normal timing of eclosion. PTTH F_0 mutants were significantly heavier and exhibited a higher incidence of diapause. This work will accelerate future studies of gene function in *O. nubilalis* and facilitate the development of similar screens in other Lepidopteran and non-model insects.

Keywords

European corn borer, Cas9, circadian, period, prothoracicotropic hormone, pigment dispersing factor receptor

Introduction

As a pest, the European corn borer (*Ostrinia nubilalis*) is responsible for substantial yield losses in corn and other crops worldwide. Although *Bacillus thuringiensis* (*Bt*) maize adoption (1996-2016) in the United States (USA) led to regional suppression of *O. nubilalis* (Dively et al. 2018), the first case of practical resistance to *Bt* Cry1F maize was identified in Nova Scotia, Canada in 2018 (Smith et al. 2019). Since then, resistance to *Bt* Cry proteins has been documented in other regions of Canada and observed on a sweet corn plot producing Cry1A.105 and Cry2Ab2 proteins in Connecticut, USA (NC 246, 2024). Although gene regions segregating with resistance have been identified (Coates et al. 2011; Coates and Siegfried 2015; Farhan et al. 2023), functional validation by gene knockout is needed to enhance sequence-based resistance monitoring (Pezzini et al. 2024) and provide mechanistic insight into cross-resistance between pyramided *Bt* toxins and foliar sprays (Abdelgaffar et al. 2021).

Beyond *Bt* resistance, prior quantitative trait locus mapping and genomic approaches have identified candidate genes associated with other traits of agroeconomic importance. For example, population differences in *O. nubilalis* female pheromone composition (Dopman et al.

2004; Lassance et al. 2010) and male preference (Unbehend et al. 2021) could alter the efficacy of passive monitoring techniques (i.e., pheromone lures) and affect the rate at which resistance alleles evolve by gene flow. Additionally, life cycle differences in generation number (voltinism; Levy et al. 2015; Kozak et al. 2019) determine the distribution and abundance of pests across space, time, and host plants. Consequently, there is a need for robust genetic techniques to probe the genetic basis of these pest traits. Considering that the function (Mackay and Anholt 2024) and evolution (Tigano and Friesen 2016; Dopman et al. 2024) of a gene depends on its genetic background, greater understanding of the genetic mechanisms underlying behavioral and ecological differences among corn borer populations is critical to effective Integrated Pest Management and Insect Resistance Management for this insect (Coates et al. 2018).

The advent of CRISPR/Cas9 genome editing has revolutionized the study of gene function in insects (Taning et al. 2017). This system utilizes a single guide RNA (sgRNA) to direct the Cas9 nuclease to specific, complementary genomic loci, where it induces a double-strand break upstream of the protospacer adjacent motif (PAM). Aberrant repair of these breaks allows for targeted disruption, insertion, or replacement of genes (Taning et al. 2017). Particularly in *O. nubilalis* and other Lepidoptera, where conventional methods like RNA interference (RNAi) are inefficient and often falter (Khajuria et al. 2011; Terenius et al. 2011; Guan et al. 2018; Cooper et al. 2021), CRISPR/Cas9 has paved the way for numerous studies of gene function. These endeavors have illuminated key mechanisms underlying diverse phenotypic traits, ranging from pigmentation and wing patterning to development and reproductive behavior (Li et al. 2021).

In this study, we demonstrate that CRISPR/Cas9 is a highly efficient and robust tool for generating heritable mutations in *O. nubilalis*. We used both single and dual sgRNAs to generate loss-of-function (LOF) mutants for three genes. Across targets, editing efficiency remained high and sufficient for streamlined studies of gene function in F_0 mutants. We also describe an approach for quantifying interactions between mutations and their genetic background. This methodology should accelerate future genetic studies in *O. nubilalis* and facilitate similar screens in other related insects.

Results and Discussion

Efficient CRISPR/Cas9-mediated mutagenesis

To assess the capacity for CRISPR/Cas9-mediated genome-editing to produce LOF mutations in *O. nubilalis*, we targeted two circadian clock genes, *period* (Konopka and Benzer 1971) and *pigment dispersing factor receptor-like* (*pdfr;* Hyun et al. 2005; Lear et al. 2005; Mertens et al. 2005). PERIOD is involved in the main transcriptional repression by CRYPTOCHROME 2 of the Lepidopteran circadian clock (reviewed in Brady et al. 2021), oscillating in abundance every ~24 hours in both entrained (light:dark, LD) and free-running (continuous darkness, DD) conditions (Hardin et al. 1990, 1992). Meanwhile, *pdfr* encodes the extracellular receptor for the neuropeptide pigment dispersing factor (PDF, Renn et al. 1999). PDF/PDFR signaling synchronizes transcriptional oscillations between clock neurons, helping maintain robust behavioral rhythms in DD (Lin et al. 2004; Peng et al. 2003; Renn et al. 1999) and adjusting these rhythms to seasonal changes in LD cycles (Ruf et al. 2021; Yoshii et al. 2009). In addition to their roles in the circadian clock network, in *O. nubilalis*, genetic differences at Z-linked *period* and *pdfr* are associated with the 14–21 day delay in spring

emergence that contributes to the life cycle difference in the number of generations per growing season between univoltine (*period*^{U}*pdfr*^{U}) and bivoltine (*period*^{B}*pdfr*^{B}) populations (Kozak et al. 2019). Univoltine prepupae also exhibit a relative increase in their propensity for seasonal diapause (Ikten et al. 2011; Yu 2022) and an earlier peak adult activity under DD (Kozak et al., 2019; Dayton & Owens *in press*).

For the CRISPR/Cas9 system, gene-specific sgRNAs were designed on the *O.nubilalis* RefSeq assembly (GCF_963855985.1) to target the coding sequences of *period* (GenBank: LOC135086880) and *pdf receptor-like* (GenBank: LOC135087024; Fig. 1, Table S1). Following oviposition by univoltine (*period*^{U}*pdfr*^{U})and bivoltine (*period*^{B}*pdfr*^{B}) females, clusters of embryos were injected with Cas9:sgRNA ribonucleoprotein (RNP) complexes in 2022 (2.5µM Cas9, 150ng/µL sgRNA). To test the effects of different sgRNA concentrations on somatic editing efficiency, eggs were injected with a higher sgRNA concentration in 2023 (2.5µM Cas9, 180ng/µL sgRNA). Typically, 7−12 embryos were injected per cluster. After hatching, injected F_0 were tracked throughout development. Most injected F_0 individuals that hatched survived to adulthood (Table 1), with an average of six F_0 per injected cluster (95CI: 3.5−9.0). Mating success did not differ significantly across sgRNAs (binomial GLM; LR $\chi^2 = 2.83$, $df = 2$, $P = 0.243$) or injection year ($\chi^2 = 0.50$, $df = 1$, $P = 0.481$; Table 1). After mating, successful F_0 parents were screened for CRISPR/Cas9-induced mutations by PCR and Sanger sequencing. Individuals were classified as somatic mutants if they exhibited >20% indel frequency, as estimated by deconvolution of Sanger sequence electropherograms (DeLay et al. 2018; Synthego Performance Analysis 2019).

CRISPR/Cas9 was highly effective. Across years and loci, 74% (95CI: 60−89%) of F_0 individuals were somatic mutants. Somatic editing efficiency was robust to the sgRNA (binomial GLM; LR $\chi^2 = 1.02$, *df* = 2, *P* = 0.601) and injection year (LR $\chi^2 = 2.57$, *df* = 1, *P* = 0.11; Table 1), and the overall efficiency was comparable to or higher than reports from other Lepidoptera (see Supporting Results). In fact, editing efficiency was so high that nearly 100% of mutations in the F_0 were heritable and transmitted to F_1 progeny (Table 1). Although the classification as "somatic mutant" is binary, the F_0 injected in 2023 (86% indels) exhibited significantly greater conversion of wildtype alleles than the F_0 from 2022 (78% indels; Wilcoxon Sign-Ranked W = 143, *P* = 0.049), underscoring a possible impact of the increase in sgRNA concentration (1.2-fold) on editing efficiency (Bassett et al., 2013; Perera et al., 2018; Wang et al., 2013).

Diverse mutations were observed at *period* (Fig. 1A) and *pdfr* (Fig. 1B). Deletions were more frequent than insertions ($\chi^2 = 14.52$, *df* = 1, *P* <0.001) and represented 82% (95CI: 37−100%) of all sequenced mutations. 78% (95CI: 64−92%) of mutations were frameshifts that produced a premature stop codon, significantly more than expected for indels within a coding sequence (i.e., two out of every three; $\chi^2 = 4.08$, *df* = 1, *P* = 0.043; Wu et al., 2018). These frameshift mutations were considered LOF null alleles, as they were predicted to encode extensively truncated proteins of PERIOD (wildtype: 1159 amino acids vs. sgRNA1: 67-89 amino acids, sgRNA2: 139-152 amino acids) and PDFR (wildtype: 431 amino acids; sgRNA1: 224 amino acids).

Mutagenesis of period but not pdfr disrupts rhythmic eclosion

To assess the phenotypic effect of *period* and *pdfr* on circadian behavior in the corn borer, we examined the timing that adult moths eclosed from their pupal case under a

summer-like photoperiod (16:8 LD hr; e.g., Markert et al. 2016). Eclosion was described in Arbitrary Zeitgeber Time (AZT), when AZT0 was the time that lights turned on. The rhythmic strength of eclosion timing was quantified by the proportion of moths who eclosed within a peak 8-hour eclosion window/gate (e.g., Ikeda et al. 2021; Liu et al. 2023; Winfree 1970). Genetic background (univoltine/bivoltine) of wildtype and mutants did not influence rhythmic strength (binomial GLM; $\chi^2 = 0.08$, $df = 1$, $P = 0.78$; AIC = 64.5; Fig. S1), so strains were combined for subsequent analyses (Fig. 2; AIC = 59.0). Most wildtype adults eclosed within an 8-hour gate from AZT15 to AZT22 in 2022 (0.83, 95CI: 0.77−0.89) and in 2023 (0.75, 95CI: 0.70−0.80; Fig. 2, Fig. S2).

Eclosion within this gate was significantly affected by mutagenesis of *per*/*pdfr* (binomial GLM; LR $\chi^2 = 40.9$, $df = 2$, $P < 1*10^{-9}$) and injection year (LR $\chi^2 = 17.4$, $df = 1$, $P < 3*10^{-5}$), with little evidence of an interaction (F = 2.87, $df = 2$, $P = 0.238$). Specifically, mutagenesis of *period* significantly decreased rhythmic strength/gating of eclosion in 2022 (Difference = -0.15, 95CI: -0.27 − -0.04; $P = 0.006$) and 2023 (-0.28, 95CI: -0.47− -0.18; $P = 1*10^{-8}$; Fig. 2). The more pronounced phenotypic effect of *period* mutation in 2023 was consistent with the higher concentration of sgRNAs and greater observed conversion of wildtype to null alleles (see above). This reduction in rhythmic strength was concordant with significantly different distribution of eclosion across the entire 24-hour distribution (Fig. S1-S2). Overall, the aberrant gating and distribution of eclosion observed for our *period* F_0 mutants recapitulated phenotypes of stable germline clock mutants in other insects. For instance, in *Drosophila melanogaster*, rhythmic strength in *period* knockouts was reduced in LD and, in the absence of light entrainment, was entirely disrupted in DD (Konopka and Benzer 1971; Qiu and Hardin 1996; Ruf

et al. 2021). In Lepidoptera, clock gene mutation similarly reduced eclosion rhythms in LD and completely abolished them in DD (*Bombyx mori*: Ikeda et al. 2021, Nartey et al. 2021; *Helicoverpa armigera*: Liu et al. 2023). Although expression of target clock genes was not measured in our study, aberrant behavioral rhythms in eclosion have been linked to disrupted molecular rhythms in circadian transcription in the brain (Markert et al. 2016; Ikeda et al. 2021; Nartey et al. 2021). Together, our mutants provide one more layer of genetic evidence highlighting the conserved essentiality of the circadian clock for the normal timing of insect eclosion (Truman and Riddiford 1974).

Unlike *period*, mutations in *pdfr* did not alter the rhythmic strength of eclosion in 2022 (0.10, 95CI: -0.09−0.28; $P = 0.575$) or 2023 (-0.11, 95CI: -0.30−0.07; $P = 0.230$; Fig. 2). These observations were similar to those in *D. melanogaster*, wherein persistent coupling of pacemaker neurons by short LD cycles (Vaze and Helfrich-Förster 2021; Yoshii et al. 2009) masks the effects of *pdf*/*pdfr* loss and behavioral rhythms remain largely unaffected (Hyun et al. 2005; Myers, Yu, and Sehgal 2003; Renn et al. 1999; Ruf et al. 2021). Instead, the consequences of *pdf/pdfr* mutations in *Drosophila* are apparent in DD, when transcription oscillations among pacemaker neurons become desynchronized (Lin et al. 2004; Peng et al. 2003; Renn et al. 1999) and output behavioral rhythms rapidly dampen (Hyun et al. 2005; Myers, Yu, and Sehgal 2003; Renn et al. 1999; Ruf et al. 2021). Additionally, *pdf*/*pdfr* mutants in *Drosophila* are unable to entrain and adjust their locomotor activity to longer photoperiods (Vaze and Helfrich-Förster 2021; Yoshii et al. 2009). Future studies on F_1 mutants in *O. nubilalis* will need to investigate the effects of *pdfr* loss on behavioral rhythms in DD and multiple LD photoperiods.

Targeted deletion of prothoracicotropic hormone by dual sgRNA injections

We expanded our investigation on the utility of CRISPR/Cas9 by simultaneously injecting multiple sgRNAs that targeted different regions of the *prothoracicotropic hormone* (*ptth*) gene. While the use of a single sgRNA successfully generated small indels at *period* and *pdfr* (Table 1, Fig. 1), we predicted that co-injecting two co-directional sgRNAs could induce large-scale LOF mutations, increase the frequency of null allele conversion within an individual (Kroll et al. 2021), and facilitate more rapid screening by PCR-based fragment size differences (e.g., Han et al. 2024; Markert et al. 2016; Zhao et al. 2023). Two co-directional sgRNAs were designed to target the 5'UTR and coding exon 1 of *ptth* (GenBank: LOC135088612; Fig. 3), immediately upstream of the region encoding the cleaved bioactive PTTH peptide (reviewed in W. Smith and Rybczynski 2012).

Cas9:dual sgRNA complexes were injected into early-stage embryos and a random sample of larvae and adults were screened for mutations (2.5µM Cas9, 180ng/µL sgRNA). Consistent with the *period* and *pdfr* injections, 72% of F_0 were somatic mutants (95CI: 56−88% , n = 32), and 59% (95CI: 36−77%, n = 23) of these mutants bore large deletions (>200 bp; Fig. 3). These deletions eliminated the original *ptth* start codon and were expected to be LOF alleles (0−24 amino acids) for PTTH (221 amino acids). Notably, three F_0 mutants from spring and fall 2023 possessed a 1 bp frameshift deletion located 200 bp downstream of the sgRNA2 PAM sequence (117 amino acids) and did not present any mutations in either sgRNA recognition sequence. Considering that homology-directed repair of double-strand breaks (DSBs) is dependent upon error-prone DNA polymerases, these distal frameshift mutations could be signatures of the hypermutation tracts known to extend from a DSB site (Deem et al. 2011; reviewed in Nambiar et al. 2022). Like *period* and *pdfr* injections in 2023, the high efficiency and

LOF mutations demonstrated in *ptth* suggested that phenotypes could be directly screened in *ptth* F_0.

ptth loss alters development in O. nubilalis

In insects, binding of the neuropeptide PTTH to its receptor on the prothoracic gland, TORSO (Rewitz et al. 2009), activates MAPK/ERK signaling and promotes synthesis of ecdysone, the developmental hormone essential for molting and metamorphosis (reviewed in W. Smith and Rybczynski 2012). A seasonally regulated shutdown in ecdysone synthesis, attributed to the absence of PTTH secretion from the brain, is broadly considered to be the neuroendocrine basis for prepupal and pupal diapause (Denlinger et al. 2012). Furthermore, considering that both secretion of PTTH is governed by a photosensitive circadian clock (e.g., Sakurai 1983; Selcho et al. 2017; Truman 1972) and a functioning circadian clock is essential for seasonal responsiveness (Liu et al. 2023), it is predicted that these two pathways converge to regulate diapause. However, the nature of this relationship between the circadian clock network, PTTH, and diapause incidence has never explicitly been validated by gene knockout.

Often, the phenotypic effect(s) of mutations at a given locus depend on their genetic background. Whereby, a general framework to identify gene interactions is to screen paired wildtype vs. mutant individuals across multiple backgrounds (Fig. 4; Mackay and Anholt 2024; Turner 2014). To measure interactions between the circadian clock and *ptth*, we explored how functionally defined circadian clock alleles in bivoltine and univoltine genetic backgrounds, specifically on the Z chromosome (i.e., *period* & *pdfr*; Kozak et al. 2019; Yu 2022), might interact with mutant *ptth* to alter development (Fig. 5). For example, reciprocal crosses between each *period* background generates two sets of F_0 offspring that differ based on whether daughters

219 inherited a bivoltine (Z^B) or univoltine (Z^U) Z chromosome from their father (note: sons are all
220 heterozygous for Z^B/Z^U; Fig. 5 *x*-axis). Since only F_0 females will differ by their genotype (e.g.,
221 Z^U/W or Z^B/W), the two populations will exhibit divergent allele frequencies on the Z
222 chromosome (i.e., Z^U ~ 0.75 vs. 0.25, Z^B ~ 0.25 vs. 0.75; Fig. 5). We injected early-stage embryos
223 from these two populations with either Cas9:dual sgRNAs (RNPs) targeting *ptth* (see Fig. 3) or a
224 controlCas9:sgRNA mixture, to respectively generate *ptth* mutant and wildtype individuals. All
225 individuals were phenotyped for diapause response under an inducing photoperiod (15:9 LD hr
226 at 23.5˚C); larvae were weighed on day 30 and phenotyped for diapause entry on day 38. Males
227 and females were analyzed together because there are no distinguishing morphological
228 features present in the prepupae. A significant interaction between sgRNA treatment and
229 candidate locus genotype on either phenotype would be consistent with strong evidence of a
230 genetic interaction (Fig. 4B; Mackay and Anholt 2024).
231 However, there was no significant evidence of an interaction between *ptth* mutation
232 and the genetic background of the Z chromosome (*period*, *pdfr*) on either mass (two-way
233 ANOVA: F = 1.46, P = 0.229; Fig. 5A) or diapause incidence (LR χ^2 = 1.40, *df* = 1, *P* = 0.237; Fig.
234 5B). Instead, mass was significantly affected by *ptth* mutation (two-way ANOVA: F = 27.66, *P* <
235 $1*10^{-5}$) and mutants (121 mg, 95CI: 112−130 mg) were 36% heavier than wildtype larvae (89
236 mg, 95CI: 81−96 mg; Fig. 5A). Genetic ablation of PTTH signaling similarly increased body size
237 and prolonged the larval growth period in *B. mori* (Uchibori-Asano et al. 2017; Zhang et al.
238 2021) and *D. melanogaster* (McBrayer et al. 2007; Rewitz et al. 2009; Shimell et al. 2018). These
239 conserved responses to PTTH loss were consistent with low ecdysteroid titers and past work
240 demonstrating that low ecdysteroidogenesis by the prothoracic gland delays developmental

timing and induces overgrowth (Colombani et al., 2005). Although ecdysone itself was not measured here, a reduced ecdysone titer in *ptth* F_0 mutants would be in line with the significant effect of *ptth* mutation on diapause incidence (binomial GLM; LR $\chi^2 = 10.4$, *df* = 1, *P* = 0.001; Fig. 5B). Whereby, the incidence of prepupal diapause by *ptth* mutants was 24% (95CI: 11−37%) higher than wildtype individuals (Wald's Z = 3.60, P < 0.001 ; Fig. 5B).

The significant additive effects of *ptth* mutation support the classic model that seasonal inhibition of PTTH secretion contributes to prepupal diapause induction (Denlinger et al., 2012). The lack of apparent epistasis between *ptth* and *period* could suggest that PTTH operates independently of or downstream of the circadian clock's role in diapause induction. However, considering that we were unable to detect known background-specific differences in diapause incidence between paired wildtype populations (Fig. 5B), our study may have been underpowered and benefitted from multiple replicate populations. Additionally, genotyping to remove the genetically invariant (Z^B/Z^U) male offspring from each population would have increased the magnitude of any effect by making *Z* chromosome allele frequencies in each F_0 population (*x*-axis, Fig. 5) fixed from each other.

Conclusions

We have demonstrated that the CRISPR/Cas9 system is a highly efficient and robust tool for generating LOF mutants in *O. nubilalis*. In the absence of visible markers or transposition reagents, we were able to generate precise mutations in three genes, recover a variety of mutant alleles, and capture phenotypic differences among F_0 mutants.

From start to finish, F_1 bearing germline mutations at a gene-of-interest can be isolated in one generation (35 days). When establishing stable mutant *O. nubilalis* lines, we recommend

that researchers plan to outcross and screen three (95% CI: 2−5) injected F_0 adults per desired LOF mutant (Table 1, Fig. 3C). This recommended number of injected F_0 adults ($n_{Injected\ Adults}$) to screen per desired LOF mutant (n_{LOF}) is based on the observed (Table 1) proportion of injected adults that mated (p_{mated}), bore somatic mutations ($p_{somatic}$) that were frameshifts ($p_{frameshift}$), and were transmitted to F_1 offspring ($n_{germline}$):

$$n_{Injected\ Adults} = \frac{n_{LOF}}{p_{germline} * p_{frameshift} * p_{somatic} * p_{mating}} = \frac{n_{LOF}}{0.98 * 0.78 * 0.74 * 0.58}$$

Depending on the lethality of the target gene and number of surviving injected adults per egg cluster, at least 0.5−1.5 egg clusters should be injected per desired LOF mutant.

Alternatively, for streamlined studies of gene function, CRISPR/Cas9 is efficient enough for immediate developmental and behavioral phenotyping of F_0 knockouts (Fig. 2, Fig. 5). To support these screens and increase the conversion of wildtype to null LOF alleles in F_0, two to three sgRNAs can be designed per coding sequence (e.g., Kroll et al. 2021; Zhu et al. 2020). See Kroll et al. (2021) for additional considerations when designing F_0 knockout screens.

Lastly, although we did not identify significant evidence of two-locus epistasis, an approach that screens paired wildtype/mutant F_0 for quantitative traits from multiple backgrounds merits further exploration (Fig. 4; Mackay and Anholt 2024; Turner 2014). Whereas this design has traditionally been limited to model organisms (e.g., *S. cerevisiae*, *C. elegans*, *D. melanogaster*), pairing modern gene-editing systems (e.g. CRISPR/Cas9) with the natural variation observed in non-model insects could revolutionize the study of genes and their modifiers on quantitative traits of agroeconomic and evolutionary interest (e.g., resistance, diapause, sexual communication).

Experimental Procedures

Insect stocks

European corn borer (*O. nubilalis*) eggs were collected from laboratory populations maintained at Tufts University (Medford, MA). These were originally derived from populations in northeastern USA, exhibit divergent allele frequencies at *period* and *pdfr*, and have repeatedly been selected and studied for different univoltine ($period^{U}pdfr^{U}$) vs. bivoltine ($period^{B}$ $pdfr^{B}$) phenotypes (e.g., Kozak et al., 2019; Dayton & Owens *in review*). Adults were mated in cages containing *ad libitum* water and covered with parchment paper for oviposition. Egg clusters were cut out, suspended over artificial corn borer diet (Southland Products, USA), and reared under 16:8 LD hr in a climate-controlled room (25.5°C, 50% RH).

sgRNA design and synthesis

CRISPR/Cas9 was leveraged to knockout *O. nubilalis* genes *period* (GenBank: LOC135086880), *pigment dispersing factor receptor-like* (*pdfr*, GenBank: LOC135087024), and *prothoracicotropic hormone* (*ptth*, GenBank: LOC135088612). Unique single guide RNA (sgRNA) targets were identified with the "$GN_{19}NGG$" guide sequence in Geneious Prime 2023.0.4. (https://www.geneious.com) and scored for predicted off-targets in the *O. nubilalis* reference genome (GenBank: GCA_008921685.1). Target-specific DNA oligos were designed to be compatible with the EnGen™ sgRNA Synthesis Kit, *S. pyogenes* (New England BioLab). Oligos were synthesized by Integrated DNA Technologies and Eton Bioscience. These sequences are provided in the Supplementary Material (Table S1).

Functional sgRNAs were synthesized following manufacturer's protocols, except fresh DTT aliquots were used and transcription was extended to 90 minutes at 37℃. sgRNAs were

purified using the Monarch RNA Cleanup Kit (10µg, New England BioLabs) and eluted in 12µL nuclease free water. sgRNAs were diluted to 600ng/µL and stored at -80℃. To form sgRNA:Cas9 (RNP) complexes, sgRNA aliquots were incubated at 70℃ for 2 minutes and mixed with 2.5µM EnGen® Spy Cas9 NLS (New England BioLabs) in injection buffer (5mM KCl, 0.1 mM sodium phosphate buffer, pH 6.8). sgRNAs were mixed to a final concentration of 150ng/µL in 2022 and 180ng/µL in 2023. The components of the control *ptth* sgRNA mixture were the same, except the *ptth* target sgRNAs were incubated at 70℃ for 8 minutes.

Embryo microinjection

Borosilicate glass capillaries (World Precision Instruments, #1B100-4; 1 mm outer dia., 0.58 mm inner dia.) were pulled on a Narishige PN-31 (Narishige Group) in 2022 (Mag_{Main} = 96, Mag_{Sub} = 33, Heat = 83) and 2023 (Mag_{Main} = 58, Mag_{Sub} = 32.8, Heat=100.7) . Needles tips were broken by scraping across forceps and retained if they exhibited a 30-55 kPa bubble pressure in water. Injections were made using a Mk1 micromanipulator (Singer Instruments) with a PLI-90 Pico-Injector Micromanipulator System (Harvard Apparatus): P_{Inj} = 30−55 kPa, P_{Bal} = 4−6 kPa, Time = 12-22 ms. Settings were adjusted within each range to inject approximately 1−3nL RNP solution per egg, as estimated by 0.01 mm calibration slide (Amscope, MR095).

Peak oviposition of *O. nubilalis* exposed to 16:8 LD hr occurs within the first two hours of darkness. Following the onset of oviposition, parchment paper containing *O. nubilalis* egg clusters (embryos) was collected every 25 minutes. The paper was cut into strips with individual egg clusters, and these were taped onto the lid of a plastic cell culture dish (Fig. S3). Under a dissecting microscope, embryos were injected within 30-60 min. of oviposition. Injections were made at a ~45-60˚ angle and the plate was rotated to access eggs. Because eggs located in the

middle of clusters were difficult to access with the micromanipulator, typically only eggs located on the perimeter were injected. Following microinjection, eggs were stored on artificial European Corn Borer Diet (Southland Products, USA) and maintained under 16:8 LD hours at 25.5˚C and 50% RH. After 24 hours, eggs were visually checked under a dissecting microscope; those without scar tissue evidence of injection were punctured to kill (Fig. S3). Approximately 7−12 eggs were typically injected per egg cluster.

Phenotyping period/pdfr injected mutants

Individuals injected with single sgRNAs targeting *period* or *pdfr* were continuously reared under 16:8 LD hours at 25.5℃ and 50% RH. Fourteen days after hatching, larvae were transferred into individual diet-containing 1.25oz plastic souffle cups (WebstaurantStore) and tracked to score survivorship. Eclosion timing of wildtype, *period* and *pdfr* mutants was monitored by the Raspberry Pi-based imaging Locomotor Activity Monitor system (iLAM; Dayton & Owens *in review*), which regularly captured images at fifteen-minute intervals. After eclosion, moths were isolated into individual mating cups and paired with two wild-type adults of the opposite sex. To score mating success, F_1 eggs were collected from each mating pair across ten days. Both F_0 and F_1 progeny were kept for follow-up genotyping.

Phenotyping ptth injected mutants

Individuals injected with Cas9:dual sgRNAs targeting *ptth* or control sgRNAs were continuously reared under diapause inducing conditions at 15:9 LD hours (23.5˚C). On Day 14, larvae were transferred into individual diet-containing 1.25 oz plastic souffle cups (WebstaurantStore). Individuals were weighed on day 30 and larvae who failed to pupate by day 38 were considered in diapause (Beck & Hanec, 1960; Mutchmor & Beckel, 1959).

Screening Mutants

DNA was extracted in 1x DirectPCR tail lysis buffer (Viagen) containing 1 µg Proteinase K (ThermoFisher Scientific, USA) in a total volume of 100 µL. Samples were incubated for 16 hr at 56°C and 85°C for 25 min. The edited region was amplified via polymerase chain reaction (PCR) containing 1X GoTaq Master Mix (Promega), 0.2µM target- gene-specific primers, and 1.5 uL of DNA extract in a 25 uL volume. Genotypes were resolved by PCR-based fragment size differences (e.g., Markert et al. 2016) or Sanger sequencing. For sequencing, PCRs were cleaned with the Exo-CIP™ Rapid PCR Cleanup Kit (New England Biolabs, USA) and Sanger-sequenced by Eton Bioscience Inc. (Boston, USA). DNA sequence electropherograms (.ab1) were trimmed and aligned in Geneious Prime 2023.0.4. (https://www.geneious.com). sgRNA:Cas9-generated indels were inferred by Synthego Inference of CRISPR Edits Analysis (ICE 2019.v3.0, Synthego Performance Analysis 2019). F_0 injected individuals bearing >20% indel frequency were classified as somatic mutants. Germline editing success was determined by genotyping progeny.

Analyses

All statistical analyses were conducted in R (R Core Team 2023). For eclosion phenotyping, the 8 hr window of the day containing the greatest number of emergences was considered the main eclosion gate (Winfree 1970; Liu et al. 2023). The main effects of sgRNA target and background on the probability of eclosing within this 8 hr gate were quantified by a binomial logistic regression. Differences in the distribution of adult eclosion were compared using Watson's U^2 test within the *circular* package (Agostinelli & Lund 2023). To evaluate evidence for epistasis between genetic background and *ptth* mutation, a linear model included the main effects of treatment (*ptth* vs. *control* sgRNA) and genetic background (Z^B vs. Z^U) on

body mass. A binomial logistic regression tested these effects on diapause incidence. For all regression models, *Anova*() from the car package (Fox & Weisberg 2019) determined whether the main effects of treatment, background, and/or their interaction were significant. Significant differences between group proportions and means were respectively evaluated by Wald's Z test and Welch's T test.

References

Abdelgaffar, Heba, Omaththage P. Perera, and Juan Luis Jurat-Fuentes. 2021. ABC Transporter Mutations in Cry1F-Resistant Fall Armyworm (*Spodoptera frugiperda*) Do Not Result in Altered Susceptibility to Selected Small Molecule Pesticides. *Pest Management Science* 77 (2): 949–55.

Agostinelli, C. and Lund, U. (2023). R package 'circular': Circular Statistics (version 0.5-0). URL https://CRAN.R-project.org/package=circular

Brady, Daniel, Alessio Saviane, Silvia Cappellozza, and Federica Sandrelli. 2021. The Circadian Clock in Lepidoptera. *Frontiers in Physiology* 12 (November): 776826.

Coates, Brad S., Erik B. Dopman, Kevin W. Wanner, and Thomas W. Sappington. 2018. Genomic Mechanisms of Sympatric Ecological and Sexual Divergence in a Model Agricultural Pest, the European Corn Borer. *Current Opinion in Insect Science* 26 (April): 50–56.

Coates, Brad S., and Blair D. Siegfried. 2015. Linkage of an ABCC Transporter to a Single QTL That Controls *Ostrinia nubilalis* Larval Resistance to the *Bacillus Thuringiensis* Cry1Fa Toxin. *Insect Biochemistry and Molecular Biology* 63 (August): 86–96.

Coates, Brad S., Douglas V. Sumerford, Miriam D. Lopez, Haichuan Wang, Lisa M. Fraser, Jeremy A. Kroemer, Terrence Spencer, et al. 2011. A Single Major QTL Controls Expression of

Larval Cry1F Resistance Trait in *Ostrinia nubilalis* (Lepidoptera: Crambidae) and Is Independent of Midgut Receptor Genes. *Genetica* 139 (8): 961–72.

Cooper, A. M.W., Song, H., Yu, Z., Biondi, M., Bai, J., Shi, X., Ren, Z., Weerasekara, S.M., Hua, D.H., Silver, K., Zhang, J., and K.Y. Zhu. 2021. Comparison of strategies for enhancing RNA interferance efficiency in *Ostrinia nubilalis*. *Pest Manag Sci.* 77 (2): 635-645.

Dayton, J.N., and A.C.S. Owens. *in press*. iLAM: imaging Locomotor Activity Monitor for circadian phenotyping of large-bodied flying insects. *Methods in Ecology and Evolution.*

Deem, Angela, Andrea Keszthelyi, Tiffany Blackgrove, Alexandra Vayl, Barbara Coffey, Ruchi Mathur, Andrei Chabes, and Anna Malkova. 2011. Break-Induced Replication Is Highly Inaccurate. *PLoS Biology* 9 (2): e1000594.

DeLay, B.D. , Corkins, M.E., Hanania, H.L., Salanga, M., Min Deng, J., Sudou, N., Taira, M., Horb, M.E., and R.K. Miller. 2018. Tissue-specific gene activation in *Xenopus laevis*: knockout of *lhx1* in the kidney with CRISPR/Cas9. *Genetics*. 208(2): 673-686.Denlinger, D. L., G. D. Yocum, and J. P. Rinehart. 2012. 10 - Hormonal Control of Diapause. In *Insect Endocrinology*, edited by Lawrence I. Gilbert, 430–63. San Diego: Academic Press.

Dively, Galen P., P. Dilip Venugopal, Dick Bean, Joanne Whalen, Kristian Holmstrom, Thomas P. Kuhar, Hélène B. Doughty, Terry Patton, William Cissel, and William D. Hutchison. 2018. Regional Pest Suppression Associated with Widespread *Bt* Maize Adoption Benefits Vegetable Growers. *Proceedings of the National Academy of Sciences* 115 (13): 3320–25.

Dopman, Erik B., Steven M. Bogdanowicz, and Richard G. Harrison. 2004. Genetic Mapping of Sexual Isolation between E and Z Pheromone Strains of the European Corn Borer (*Ostrinia nubilalis*). *Genetics* 167 (1): 301–9.

Dopman, Erik B., Kerry L. Shaw, Maria R. Servedio, Roger K. Butlin, and Carole M. Smadja. 2024. Coupling of Barriers to Gene Exchange: Causes and Consequences. *Cold Spring Harbor Perspectives in Biology*, January. https://doi.org/10.1101/cshperspect.a041432.

Farhan, Yasmine, Jocelyn L. Smith, Michael G. Sovic, and Andrew P. Michel. 2023. Genetic Mutations Linked to Field-Evolved Cry1Fa-Resistance in the European Corn Borer, *Ostrinia nubilalis*. *Scientific Reports* 13 (1): 8081.

Fox J, Weisberg S (2019). *An R Companion to Applied Regression*, Third edition. Sage, Thousand Oaks CA.

Guan, Ruo-Bing, Hai-Chao Li, Yu-Jie Fan, Shao-Ru Hu, Olivier Christiaens, Guy Smagghe, and Xue-Xia Miao. 2018. A Nuclease Specific to Lepidopteran Insects Suppresses RNAi. *The Journal of Biological Chemistry* 293 (16): 6011–21.

Han, Wei-Kang, Feng-Xian Tang, Yang-Yang Yan, Yan Wang, Yi-Xi Zhang, Na Yu, Kan Wang, and Ze-Wen Liu. 2024. An OBP Gene Highly Expressed in Non-Chemosensory Tissues Affects the Phototaxis and Reproduction of *Spodoptera frugiperda*. *Insect Molecular Biology* 33 (1): 81–90.

Hardin, P. E., J. C. Hall, and M. Rosbash. 1990. Feedback of the *Drosophila* Period Gene Product on Circadian Cycling of Its Messenger RNA Levels. *Nature* 343 (6258): 536–40.

Hardin, P.E., J.C. Hall, and M. Rosbash. 1992. Circadian Oscillations in Period Gene mRNA Levels Are Transcriptionally Regulated. *Proceedings of the National Academy of Sciences* 89 (24): 11711–15.

Hyun, Seogang, Youngseok Lee, Sung-Tae Hong, Sunhoe Bang, Donggi Paik, Jongkyun Kang, Jinwhan Shin, et al. 2005. *Drosophila* GPCR Han Is a Receptor for the Circadian Clock

Neuropeptide PDF. *Neuron* 48 (2): 267–78.

Ikeda, Kento, Takaaki Daimon, Kunihiro Shiomi, Hiroko Udaka, and Hideharu Numata. 2021. Involvement of the Clock Gene Period in the Photoperiodism of the Silkmoth *Bombyx mori*. *Zoological Science* 38 (6): 523–30.

Ikten, Cengiz, Steven R. Skoda, Thomas E. Hunt, Jaime Molina-Ochoa, and John E. Foster. 2011. Genetic Variation and Inheritance of Diapause Induction in Two Distinct Voltine Ecotypes of *Ostrinia nubilalis* (Lepidoptera: Crambidae). *Annals of the Entomological Society of America* 104 (3): 567–75.

Khajuria, C., Buschman, L.L., Chen, M.S., Siegfried, B.D., and K.Y. Zhu. 2011. Identification of a novel aminopeptidase P-like gene (OnAPP) possibly invovled in Bt toxicity and resistance in a major corn pest (*Ostrinia nubilalis*). PLoS ONE 6(8): e23983.

Konopka, R. J., and S. Benzer. 1971. Clock Mutants of *Drosophila* Melanogaster. *Proceedings of the National Academy of Sciences of the United States of America* 68 (9): 2112–16.

Kozak, Genevieve M., Crista B. Wadsworth, Shoshanna C. Kahne, Steven M. Bogdanowicz, Richard G. Harrison, Brad S. Coates, and Erik B. Dopman. 2019. Genomic Basis of Circannual Rhythm in the European Corn Borer Moth. *Current Biology: CB* 29 (20): 3501-3509.e5.

Kroll, François, Gareth T. Powell, Marcus Ghosh, Gaia Gestri, Paride Antinucci, Timothy J. Hearn, Hande Tunbak, et al. 2021. A Simple and Effective F0 Knockout Method for Rapid Screening of Behaviour and Other Complex Phenotypes. *ELife* 10 (January). https://doi.org/10.7554/eLife.59683.

Lassance, Jean-Marc, Astrid T. Groot, Marjorie A. Liénard, Binu Antony, Christin Borgwardt,

Fredrik Andersson, Erik Hedenström, David G. Heckel, and Christer Löfstedt. 2010. Allelic Variation in a Fatty-Acyl Reductase Gene Causes Divergence in Moth Sex Pheromones. *Nature* 466 (7305): 486–89.

Lear, Bridget C., C. Elaine Merrill, Jui-Ming Lin, Analyne Schroeder, Luoying Zhang, and Ravi Allada. 2005. A G Protein-Coupled Receptor, Groom-of-PDF, Is Required for PDF Neuron Action in Circadian Behavior. *Neuron* 48 (2): 221–27.

Levy, R. C., G. M. Kozak, C. B. Wadsworth, B. S. Coates, and E. B. Dopman. 2015. Explaining the Sawtooth: Latitudinal Periodicity in a Circadian Gene Correlates with Shifts in Generation Number. *Journal of Evolutionary Biology* 28 (1): 40–53.

Li, Jiang-Jie, Yan Shi, Ji-Nan Wu, Hao Li, Guy Smagghe, and Tong-Xian Liu. 2021. CRISPR/Cas9 in Lepidopteran Insects: Progress, Application and Prospects. *Journal of Insect Physiology* 135 (October): 104325.

Lin, Yiing, Gary D. Stormo, and Paul H. Taghert. 2004. The Neuropeptide Pigment-Dispersing Factor Coordinates Pacemaker Interactions in the *Drosophila* Circadian System. *The Journal of Neuroscience: The Official Journal of the Society for Neuroscience* 24 (36): 7951–57.

Liu, Xiaoming, Limei Cai, Lin Zhu, Zhiqiang Tian, Zhongjian Shen, Jie Cheng, Songdou Zhang, Zhen Li, and Xiaoxia Liu. 2023. Mutation of the Clock Gene Timeless Disturbs Diapause Induction and Adult Emergence Rhythm in *Helicoverpa armigera*. *Pest Management Science* 79 (5): 1876–84.

Mackay, Trudy F. C., and Robert R. H. Anholt. 2024. Pleiotropy, Epistasis and the Genetic Architecture of Quantitative Traits. *Nature Reviews. Genetics*, April.

https://doi.org/10.1038/s41576-024-00711-3.

Markert, Matthew J., Ying Zhang, Metewo S. Enuameh, Steven M. Reppert, Scot A. Wolfe, and Christine Merlin. 2016. Genomic Access to Monarch Migration Using TALEN and CRISPR/Cas9-Mediated Targeted Mutagenesis. *G3 (Bethesda, Md.)* 6 (4): 905–15.

McBrayer, Zofeyah, Hajime Ono, Maryjane Shimell, Jean-Philippe Parvy, Robert B. Beckstead, James T. Warren, Carl S. Thummel, Chantal Dauphin-Villemant, Lawrence I. Gilbert, and Michael B. O'Connor. 2007. Prothoracicotropic Hormone Regulates Developmental Timing and Body Size in *Drosophila*. *Developmental Cell* 13 (6): 857–71.

Mertens, Inge, Anick Vandingenen, Erik C. Johnson, Orie T. Shafer, W. Li, J. S. Trigg, Arnold De Loof, Liliane Schoofs, and Paul H. Taghert. 2005. PDF Receptor Signaling in *Drosophila* Contributes to Both Circadian and Geotactic Behaviors. *Neuron* 48 (2): 213–19.

Mutchmor, J.A., and W.E. Beckel. 1959. Some factors affecting diapause in the European corn borer, *Ostrinia nubilalis* (Hbn.) (Lepidoptera: Pyralidae). *Canadian Journal of Zoology* 37: 161-168.

Myers, Edith M., Jiujiu Yu, and Amita Sehgal. 2003. Circadian Control of Eclosion: Interaction between a Central and Peripheral Clock in *Drosophila* Melanogaster. *Current Biology: CB* 13 (6): 526–33.

Nambiar, Tarun S., Lou Baudrier, Pierre Billon, and Alberto Ciccia. 2022. CRISPR-Based Genome Editing through the Lens of DNA Repair. *Molecular Cell* 82 (2): 348–88.

Nartey, Moses Addo, Xia Sun, Sheng Qin, Cheng-Xiang Hou, and Mu-Wang Li. 2021. CRISPR/Cas9-Based Knockout Reveals That the Clock Gene Timeless Is Indispensable for Regulating Circadian Behavioral Rhythms in *Bombyx mori*. *Insect Science* 28 (5): 1414–

25.

NC. 2024. NC246: Ecology and Management of Arthropods in Corn. In: https://nimss.org/projects/view/mrp/outline/18695.

Peng, Ying, Dan Stoleru, Joel D. Levine, Jeffrey C. Hall, and Michael Rosbash. 2003. *Drosophila* Free-Running Rhythms Require Intercellular Communication. *PLoS Biology* 1 (1): E13.

Pezzini, Daniela, Katherine L. Taylor, Dominic D. Reisig, and Megan L. Fritz. 2024. Cross-Pollination in Seed-Blended Refuge and Selection for Vip3A Resistance in a Lepidopteran Pest as Detected by Genomic Monitoring. *Proceedings of the National Academy of Sciences* 121 (13): e2319838121.

Qiu, J., and P. E. Hardin. 1996. Developmental State and the Circadian Clock Interact to Influence the Timing of Eclosion in *Drosophila* Melanogaster. *Journal of Biological Rhythms* 11 (1): 75–86.

Renn, S. C., J. H. Park, M. Rosbash, J. C. Hall, and P. H. Taghert. 1999. A Pdf Neuropeptide Gene Mutation and Ablation of PDF Neurons Each Cause Severe Abnormalities of Behavioral Circadian Rhythms in *Drosophila*. *Cell* 99 (7): 791–802.

Rewitz, Kim F., Naoki Yamanaka, Lawrence I. Gilbert, and Michael B. O'Connor. 2009. The Insect Neuropeptide PTTH Activates Receptor Tyrosine Kinase Torso to Initiate Metamorphosis. *Science* 326 (5958): 1403–5.

Ruf, Franziska, Oliver Mitesser, Simon Tii Mungwa, Melanie Horn, Dirk Rieger, Thomas Hovestadt, and Christian Wegener. 2021. Natural Zeitgebers Under Temperate Conditions Cannot Compensate for the Loss of a Functional Circadian Clock in Timing of a Vital Behavior in *Drosophila*. *Journal of Biological Rhythms* 36 (3): 271–85.

527 Sakurai, Syo. 1983. Temporal Organization of Endocrine Events Underlying Larval-Larval Ecdysis
528 in the Silkworm, *Bombyx mori*. *Journal of Insect Physiology* 29 (12): 919–32.
529 Selcho, Mareike, Carola Millán, Angelina Palacios-Muñoz, Franziska Ruf, Lilian Ubillo, Jiangtian
530 Chen, Gregor Bergmann, et al. 2017. Central and Peripheral Clocks Are Coupled by a
531 Neuropeptide Pathway in *Drosophila*. *Nature Communications* 8 (May): 15563.
532 Shimell, Maryjane, Xueyang Pan, Francisco A. Martin, Arpan C. Ghosh, Pierre Leopold, Michael
533 B. O'Connor, and Nuria M. Romero. 2018. Prothoracicotropic Hormone Modulates
534 Environmental Adaptive Plasticity through the Control of Developmental Timing.
535 *Development* 145 (6). https://doi.org/10.1242/dev.159699.
536 Smith, Jocelyn L., Yasmine Farhan, and Arthur W. Schaafsma. 2019. Practical Resistance of
537 *Ostrinia nubilalis* (Lepidoptera: Crambidae) to Cry1F Bacillus Thuringiensis Maize
538 Discovered in Nova Scotia, Canada. *Scientific Reports* 9 (1): 1–10.
539 Smith, Wendy, and Robert Rybczynski. 2012. 1 - Prothoracicotropic Hormone. In *Insect*
540 *Endocrinology*, edited by Lawrence I. Gilbert, 1–62. San Diego: Academic Press.
541 Synthego Performance Analysis, ICE Analysis. 2019. v3.0. Synthego.
542 Taning, Clauvis Nji Tizi, Benigna Van Eynde, Na Yu, Sanyuan Ma, and Guy Smagghe. 2017.
543 CRISPR/Cas9 in Insects: Applications, Best Practices and Biosafety Concerns. *Journal of*
544 *Insect Physiology* 98 (April): 245–57.
545 Terenius, Olle, Alexie Papanicolaou, Jennie S. Garbutt, Ioannis Eleftherianos, Hanneke Huvenne,
546 Sriramana Kanginakudru, Merete Albrechtsen, et al. 2011. RNA Interference in
547 Lepidoptera: An Overview of Successful and Unsuccessful Studies and Implications for
548 Experimental Design. *Journal of Insect Physiology* 57 (2): 231–45.

549 Tigano, Anna, and Vicki L. Friesen. 2016. Genomics of Local Adaptation with Gene Flow.
550 *Molecular Ecology* 25 (10): 2144–64.
551 Truman, J. W. 1972. Physiology of Insect Rhythms: II. The Silkmoth Brain as the Location of the
552 Biological Clock Controlling Eclosion. *Journal of Comparative Physiology*.
553 https://link.springer.com/article/10.1007/BF00693553.
554 Truman, J. W., and L. M. Riddiford. 1974. Physiology of Insect Rhythms: III. The Temporal
555 Organization of the Endocrine Events Underlying Pupation of the Tobacco Hornworm.
556 *The Journal of Experimental Biology* 60 (2): 371–82.
557 Turner, Thomas L. 2014. Fine-Mapping Natural Alleles: Quantitative Complementation to the
558 Rescue. *Molecular Ecology* 23 (10): 2377–82.
559 Uchibori-Asano, Miwa, Takumi Kayukawa, Hideki Sezutsu, Tetsuro Shinoda, and Takaaki
560 Daimon. 2017. Severe Developmental Timing Defects in the Prothoracicotropic
561 Hormone (PTTH)-Deficient Silkworm, *Bombyx mori*. *Insect Biochemistry and Molecular*
562 *Biology* 87 (August): 14–25.
563 Unbehend, Melanie, Genevieve M. Kozak, Fotini Koutroumpa, Brad S. Coates, Teun Dekker,
564 Astrid T. Groot, David G. Heckel, and Erik B. Dopman. 2021. Bric à Brac Controls Sex
565 Pheromone Choice by Male European Corn Borer Moths. *Nature Communications* 12
566 (1): 2818.
567 Vaze, Koustubh M., and Charlotte Helfrich-Förster. 2021. The Neuropeptide PDF Is Crucial for
568 Delaying the Phase of *Drosophila's* Evening Neurons under Long Zeitgeber Periods.
569 *Journal of Biological Rhythms* 36 (5): 442–60.
570 Winfree, A. T. 1970. Integrated View of Resetting a Circadian Clock. *Journal of Theoretical*

Biology 28 (3): 327–74.

Yoshii, Taishi, Corinna Wülbeck, Hana Sehadova, Shobi Veleri, Dominik Bichler, Ralf Stanewsky, and Charlotte Helfrich-Förster. 2009. The Neuropeptide Pigment-Dispersing Factor Adjusts Period and Phase of *Drosophila*'s Clock. *The Journal of Neuroscience: The Official Journal of the Society for Neuroscience* 29 (8): 2597–2610.

Yu, Yue. 2022. Genetic Basis of Seasonal Timing in Two Moth Species. Ph.D. dissertation. Tufts University.

Zhang, Zhong-Jie, Xiao-Jing Liu, Ye Yu, Fang-Ying Yang, and Kai Li. 2021. The Receptor Tyrosine Kinase Torso Regulates Ecdysone Homeostasis to Control Developmental Timing in *Bombyx mori*. *Insect Science* 28 (6): 1582–90.

Zhao, Jing, Yongan Tan, Yiping Jiang, Keyan Zhu-Salzman, and Liubin Xiao. 2023. CRISPR/Cas9-Mediated Methoprene-Tolerant 1 Knockout Results in Precocious Metamorphosis of Beet Armyworm (*Spodoptera Exigua*) Only at the Late Larval Stage. *Insect Molecular Biology* 32 (2): 132–42.

Zhu, Guan-Heng, Shankar C. R. R. Chereddy, Jeffrey L. Howell, and Subba Reddy Palli. 2020. Genome Editing in the Fall Armyworm, *Spodoptera frugiperda*: Multiple SgRNA/Cas9 Method for Identification of Knockouts in One Generation. *Insect Biochemistry and Molecular Biology* 122 (July): 103373.

Tables

Table 1. CRISPR/Cas9-induced mutagenesis in *O. nubilalis*. Single Cas9:sgRNA mixtures targeting the *period* and *pigment-dispersing factor receptor-like* (*pdfr*) genes were microinjected into *O. nubilalis* eggs. Percent survival was not determined (nd) in 2023. The percentage of successful matings was determined from a subset (n) of the total individuals that survived to adulthood. Similarly, the percentage of somatic mutants is based on the number of genotyped (n) fertile F_0 adults that presented somatic mosaicism >20%. Germline mutation rate corresponds to the percentage of F_1 progeny with a mutated allele of the total progeny genotyped (n). Grand means with 95% confidence interval are provided in the bottom row.

	Target (sgRNA)	Injected Clusters	Survived to Adult, N (%)	% Successful Matings (n)	% Somatic F_0 Mutants (n)	% Germline F_1 Mutation Rate (n)
2022	*period* (1)	12	67 (81%)	49% (51)	58% (19)	86% (7)
	period (2)	12	50 (65%)	48% (42)	80% (15)	100% (4)
	pdfr (1)	4	11 (52%)	78% (9)	71% (7)	100% (3)
2023	*period* (1)	8	56 (nd)	63% (27)	93% (15)	100% (5)
	period (2)	8	79 (nd)	51% (43)	84% (19)	100% (5)
	pdfr (1)	4	33 (nd)	64% (14)	60% (5)	100% (2)
			Grand mean:	58% (47−71%)	74% (60−89%)	98% (92−100%)

Figures

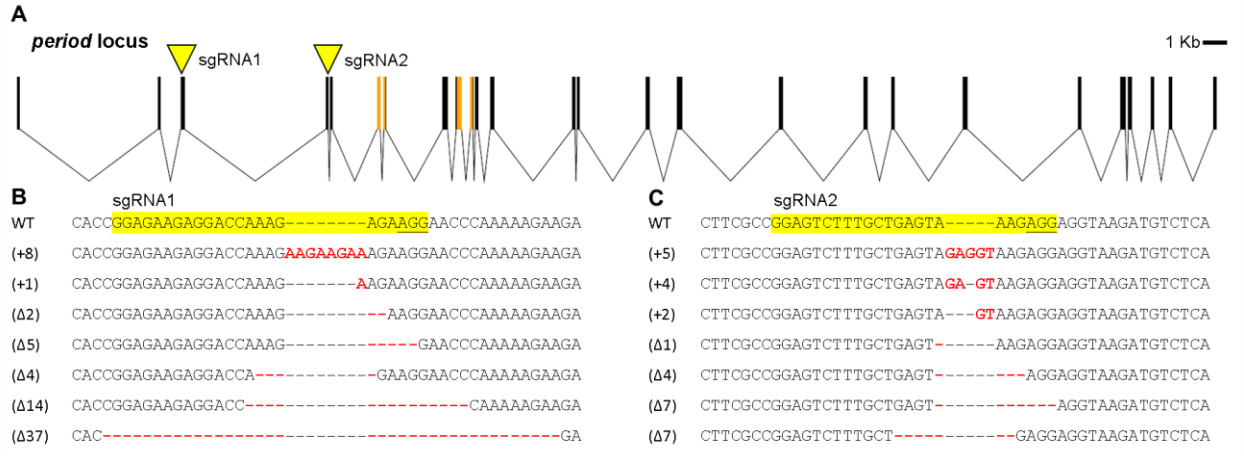

Fig. 1. CRISPR/Cas9-mediated mutagenesis of *O. nubilalis* genes *period* and *pdfr*. (A) (Top) Exon-intron gene model of the *period* coding sequence (exons 2-27; GenBank: LOC135086880). Yellow triangles indicate approximate positions of sgRNA recognition sequences in exon 4 and exon 5. Predicted PAS domains are colored orange. (Bottom) Representative frameshift mutations induced by microinjection of single sgRNA1:Cas9 and sgRNA2:Cas9 mixtures. The protospacer adjacent motif (PAM site, 5'-NGG-3') within the highlighted sgRNA target sequence is underlined. Compared to the wildtype (WT) sequence, red dashes and bases denote deletions and insertions, respectively. (B) (Top) Exon-intron gene model of the *pdf receptor-like* (*pdfr*) coding sequence (exons 2-11; GenBank: LOC135087024). Yellow triangles indicate the sgRNA recognition sequences in exon 7 and the predicted C-terminal domain is in orange. (Bottom) Representative induced mutations annotated as in (A).

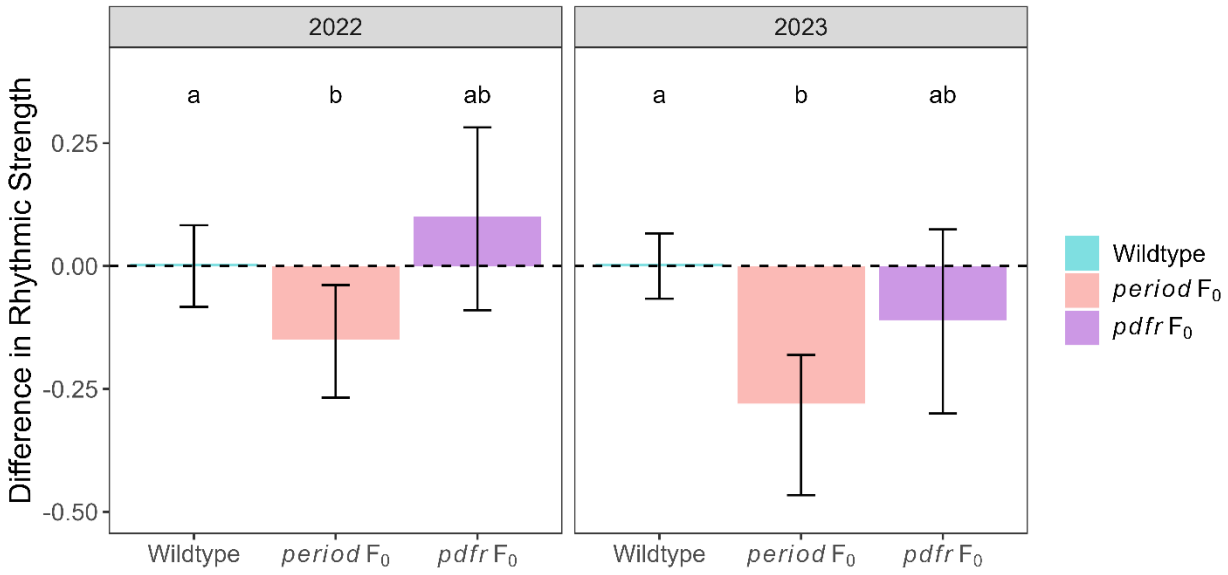

Fig. 2. *period* but not *pdfr* mutagenesis reduces rhythmic strength in wildtype eclosion timing. Wildtype *Ostrinia nubilalis* were injected with Cas9:sgRNA targeting *period* and *pdfr* in 2022 and 2023. Eclosion of uninjected wildtype and injected F_0 adults exposed to 16L:8D hr were monitored in Arbitrary Zeitgeber Time (AZT). Rhythmic strength was quantified as the proportion of adults that eclosed from their pupal case between AZT15 and AZT22, the 8 hr window encapsulating the time most wildtype adults emerge. The main effects of treatment and injection year on the rhythmic strength were modeled by a binomial logistic regression (AIC = 59.0, *df* = 5). Within each year, the difference in rhythmic strength (a proportion) between wildtype and the *period* vs. *pdfr* F_0 was determined. Significant differences between groups were measured by Wald's test and do not encompass zero (i.e. no difference). Letters denote significant differences among groups (P <0.05), with B-Y adjustment for multiple comparisons. Error bars represent 95% confidence intervals

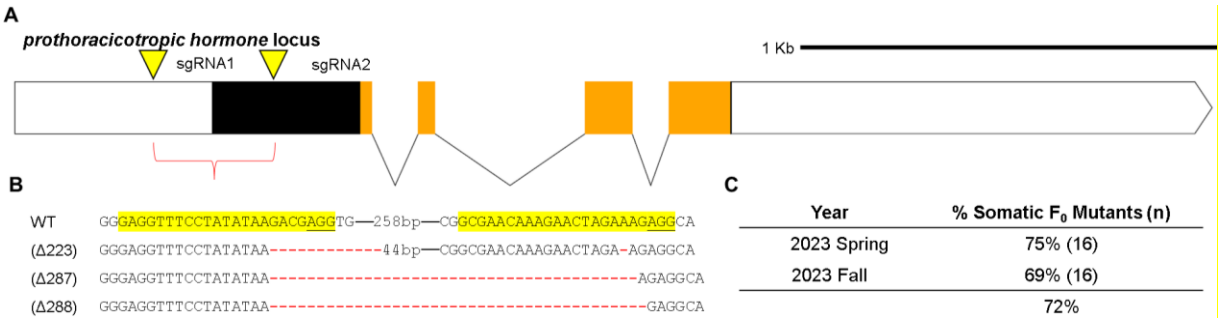

632

633 **Fig. 3. Efficient deletion of *prothoracicotropic hormone* by dual sgRNAs.** (A) (Top) Exon-intron

634 gene model of *prothoracicotropic hormone* (*ptth*) (GenBank: LOC135088612). Yellow triangles

635 indicate the sgRNA recognition sequences in the 5'-UTR and exon 1 and the red bracket

636 denotes the predicted interior deletion (Δ285 bp). The exons corresponding to the predicted

637 bioactive PTTH peptide are in orange. (B) (Bottom) Representative frameshift mutations

638 induced by microinjection of dual sgRNA1+sgRNA2:Cas9. The protospacer adjacent motif (PAM

639 site, 5'-NGG-3') of the highlighted sgRNA target sequences are underlined. Red dashes denote

640 deletions compared to the wildtype (WT) reference. (C) The percentage of somatic mutants is

641 based on the number (n) of genotyped F_0 individuals that presented somatic mosaicism >20%.

642

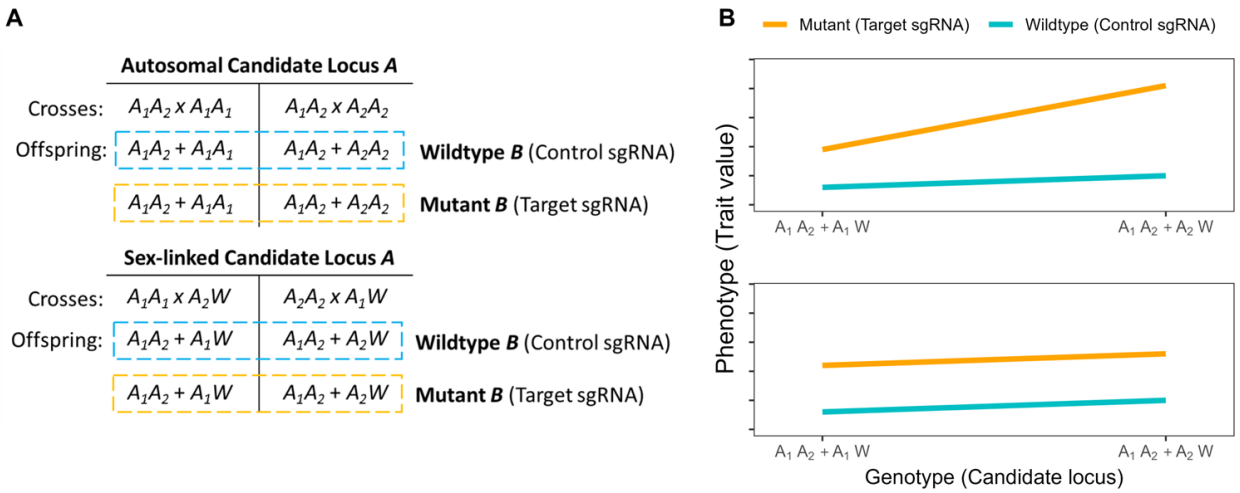

Fig. 4. Test for two-locus epistasis between *A* and *B* for a quantitative trait. (A) Interactions between alleles at candidate locus *A* and target locus *B* are measured in F_0 offspring derived from reciprocal crosses. Given a similar number of offspring from each genotype, all polymorphic alleles among F_0 have frequencies of 0.50, except for locus *A* (e.g., A_2 ~ 0.25 vs. A_2 ~ 0.75). To generate wildtype *B* (control) or loss-of-function (LOF) *B* mutants (sgRNA), early-stage F_0 embryos are respectively injected with a control Cas9:sgRNA or a functional Cas9:sgRNA mixture. (B) The phenotype of the quantitative trait is plotted against two paired populations with different genotypes at the *A* locus, and separately for wildtype *B* (blue) and mutant *B* (orange). Epistasis between loci is estimated by fitting a statistical model that includes the main effects of genotype for candidate locus *A* (A_1 or A_2), LOF mutations at *B* and their interaction. (B) (Top) A statistically significant interaction provides strong evidence for epistasis, in which the additive effect of locus *B* is greater in individuals from the A_2W background. (B) (Bottom) Significant main effects of *A* genotype and *B* mutation with no interaction reveal separate additive contributions of locus *A* and *B*, with no epistasis.

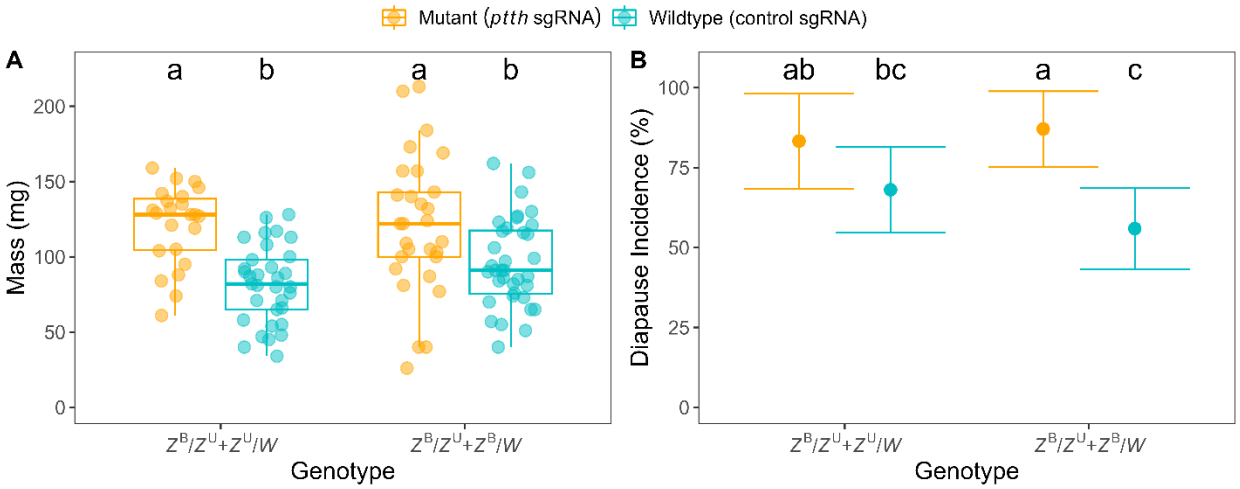

Fig. 5. Test for two-locus epistasis between *ptth* mutants from univoltine and bivoltine backgrounds. (A) Reciprocal crosses between univoltine (Z^U) and bivoltine (Z^B) individuals generated two F_0 populations. With a similar number of male and female offspring, each F_0 population should exhibit a different allele frequency at *Z*-linked genes (Z^U ~ 0.75 vs. 0.25 and Z^B ~ 0.25 vs. 0.75; See Figure 4A). Early-stage F_0 embryos were injected with functional Cas9:sgRNA targeting *prothoracicotropic hormone* (*ptth*) or control Cas9:sgRNA to respectively generate loss-of-function (LOF) mutant *ptth* or wildtype *ptth* individuals. Following injection, F_0 were raised in 15L:9D hr and phenotyped for (A) body mass (day 30) and (B) diapause incidence (day 38). The phenotype of the quantitative trait is plotted against two population backgrounds for the *Z* chromosome, and separately for wildtype (blue) and mutant *ptth* (orange). Epistasis was estimated by fitting a model with main effects of *Z* background, *ptth* mutation, and their interaction on mass (normal distribution) or diapause incidence (binomial distribution). Differences between groups were measured by (A) Welch's t-test and (B) Wald's test. Letters denote significant differences among groups (P <0.05), with a B-Y adjustment for multiple comparisons. Bars in panel (B) denote 95% confidence intervals.

676